INFN/AE - 77/8
30 maggio 1977

BEAM STUDY ON THE 125-MeV CHANNEL OF THE CERN 600-MeV SYNCHROCYCLOTRON

N. Grion and G. Musuruana

Istituto di Fisica, Università di Trieste, Trieste, Italia
Istituto Nazionale di Fisica Nucleare, Sezione di Trieste, Italia

A B S T R A C T

An analysis of the π^- beam at the 125-MeV channel of the CERN 600-MeV Synchrocyclotron is reported. The Position of the pion producing internal target and the beam transport magnetic system have been investigated in order to obtain a π^- beam suitable for π^- absorption at rest experiments.

1. - INTRODUCTION

In this report we present the results of a series of measurements carried out by our group at the CERN 600-MeV synchrocyclotron (SC) in order to investigate the beam composition of the 125-MeV nominal energy pion channel.

The need of such measurements was justified by the following reasons related to an experiment on the negative pion absorption at rest in light nuclei, which our group is planning to perform at the SC (Ref.1). For such experiment the stopping rate of negative pions in rather thin tragets ($0.2 \div 0.3$ gr/cm^2) should be the highest as possible. To meet this requirement the incoming pion beam should have:

1) a low energy in order to reduce as much as possible the pion losses due to nuclear interactions in the energy degrading material;

2) a spread in momentum as low as possible in order to enhance the stopping rate in thin targets;

3) a contamination of muons and electrons (always present in such beams) as small as possible in order to reduce any possible source of background in the experiment.

This conditions are rather well satisfied by the pion beam available at the LEPC channel of the SC. Unfortunately, this channel conveys negative pion beams for field-up conditions of the machine, which means clockwise circulation of the internal proton beam, so that the sharing of the extracted proton beam is not possible.

This reason and also the lack of sufficient space in the experimental area in front of the LEPC channel (neutron room) forced us to explore other possibilities for having a beam with the required characteristics.

After having excluded the use of pions produced by external targets in the proton room because of the presence of cumbersome apparatus in this room, a solution of comporomise was realized at the 125-MeV channel in the neutron room with field-down conditions of the machine so as to make possible the sharing of the machine-time with groups using the extracted proton beam. We succeeded in obtaining a satisfactory pion beam at this channel through the proper choice of the pion producing internal

target position and of the corresponding set-up of the magnetic transport system of the beam.

The most critical element of this system is the inflector magnet (MH1) through which, by adjusting its position and field, low energy pions can be injected into the channel in greater number than that obtained by the action of the fringing field of the machine only. In fact this method works normally with machine field-up conditions.

2. - EXPERIMENTAL GEOMETRY

The geometric arrangement of the experimental set-up is schematically represented in Figure 1.

The experimental procedure consisted in measuring (a) the time-of-flight spectrum of the particles in the beam and determining thereform the momentum spread of the pions, and (b) the differential range-curve for evaluating the stopping rate of pions. All these measurements have been performed for various settlements of the position of the pion producing internal target, and also of the beam transport magnet currents. The data relative to field-down conditions (meas. n° 1, 3, 4, 5) and, for the sake of comparison, to fiel-up conditions (meas. n° 2) of the machine are reported in Table I.

In the beam transport system, apart from the inflector magnet (MH1), there are also two quadrupole lenses (LC1 & LC2) having the function of focalizing the beam on a collimator of variable aperture. This aperture determine both the intensity and the momentum spread of the beam. The collimator can be also condidered as a virtual object for the rest of the beam transport system which, beside the focalizing quadrupoles LB30, LB31, LB40, LB25, containes also a momentum analyser magnet (MC3). This last magnet is set for a 35° deflection of negatively charged particles.

The time-of-flight was measured by two plastic scintillator counters, C_0 and C_2, coupled at the lateral sides to XP2230 photomultipliers by means of adiabatic lucite light pipes.

The other detectors C_1, C_3, C_4 together with C_2 formed a beam telescope with C_1 used ad beam monitor, C_3 as a simulated target of 0.2 gr/cm^2

and C_4 as an anticoicidence counter to detect the pions stopped in C_3. The dimensions of all the counters are reported in Figure 2.

The C_4 anticoincidence counter was also coupled to two photomultipliers (EMI9815b) because of the need of having a nearly 100% efficiency for charged particles combined with a rather thin thickness in order to have the minimum possible efficiency for neutron detection, as required by the planned experiment.

3. - EXPERIMENTAL PROCEDURE

The electronics used for the measurements is shown in the block diagram of Figure 3.

The signals from the photomultipliers connected to the counters C_0 and C_2 are shaped by ORTEC 454 Timing Filter Amplifiers in order to get the best timing with the ORTEC 473 Constant Fraction Timing Discriminators. The use of the 454 TFA has also the advantage of allowing a multiple use of the output signals without heavy losses and deformations of their shape (ReF. 2).

The best timing performances have been reached by using the 473 CFTD in the EXT shape position, by a suitable choice of the delay cable, instead of using them in the SCINT position.

The signals from either the counters C_0 and C_2 were furthermore sent into a Mean Timer circuit. This circuit has the function of compensating the time differences due to the different light paths in the scintillator depending on the detection point in it (Ref. 3).

By a proper adjustment of all the parameters involved in this circuitry it was possible to achieve time resolutions of the order of 350 psec.

All of the photomultipliers were supplied with the same high-voltage value in order to have the same time dispersion in them; the differences in the pulse heights were compensated by suitable attenuators.

A typical t-o-f spectrum is shown in Figure 4. The distance between C_0 and C_2 used for this spectrum measurement was equal to 4.80 meters,

being limitated by the availability of the experimental area. Such flight-path allowed us to get a good identification of the composition of the beam but, unfortunately, was not enough to deduce the momentum spread of the pions simply by looking at the FWHM in the time-of-flight spectrum. This was possible in previous measurements with pion energies of about 80 MeV at the LEPC channel (Ref. 3). Anyway the FWHM could give a rough estimation (4.5%) of the true value (6.0%) deduced from the range curve, as indicated in Figure 5.

The logic part of the electronics was made by generating logic pulses from the linear signals of counters C_1, C_2, C_3, and C_4, by means of fast discrimator, and feeding these pulses to coincidence circuits. A double coincidence $C_3 \times C_4$ gave the signals really needed to veto the signals from the coincidence $C_1 \times C_2 \times C_3$ so that $C_1 \times C_2 \times C_3 \times \bar{C}_4$ was the signal to be used in the determination of the range curve. (The coincidences $C_1 \times C_2 \times C_3$ gave the integral and the $C_1\ C_2\ C_3\ \bar{C}_4$ the differential range-curve). The same signal was also used to gate the Time-to-amplitude converter in order to measure the time-of-flight spectrum corresponding to pions stopped in the simulated target C_3 (Figure 6). Clearly this spectrum shoud be a peak having a width determined by the spread in time of the electronic system because only pions of very well defined velocity can be stopped in a plastic scintillator only 2 mm thick. But, as seen from Figure 6, in the spectrum is also present a peak which corresponds to electrons apparently stopped in C_3. Since such an event is physically impossible, the correct interpretation is that electrons scattered at small angles in the absorber pass across the light-guides of the counter C_3 producing a signal by Cerenkov radiation, so as to simulate a stopping event in this counter in all those cases in which these electrons are not detected by the anticounter C_4 because of geometric reasons.

By gating the scaler which counts the $C_1 \times C_2 \times C_3 \times \bar{C}_4$ events with logic signals furnished by an ORTEC 420 Timing Single Channel Analyser which selects from the t-o-f spectrum of the particles stopped in C_3 the part corresponding to stopped pions only (Figure 7), one can determine the true range curve for pions (Figure 8).

Asymmetries in the range curves are to be attributed to an asymmetry already present in the magnet transversal curve (Figure 9). This asymmetry

can be easly removed by acting on the magnet MCH, the purpose of which is just to direct the beam towards the collimator.

So, one may bear in mind that it is important to reduce as much the electron contamination in the beam, but, on the other hand, that it is possible to have the exact number of pions stopped in a target by the use of the time-of-flight spectrum for the stopped beam.

From Figure 8 it is clear that the correction for electrons is uniformily distributed over the entire range curve and lowers the continuous level of it. At the maximum of the range curve this level produces a background of apparently stopped pions which in reality is due to pion interactions in the counter C_3 or in the last layers of the absorber and producing no signal from the counter C_4. This is a physical background which becomes increasingly important at higher energies of the incoming beam, a fact which explains the need of using the lowest possible energy.

The background represented by $C_1 \times C_2 \times C_3 \times \bar{C}_4$ events that do not correspond to pions stopped in the true target, will be eliminated almost completely in the planned experiment by taking the t-o-f spectrum relative to all the $C_1 \times C_2 \times C_3 \times \bar{C}_4$ events with the true target in and out of the beam, and then by selecting those events corresponding to the peak which appears in the t-o-f spectrum when the true target is in.

4. - EXPERIMENTAL RESULTS

The significant results of our measurements are reported in Table I, where the various parameters are clearly indicated.

It is worthwhile to do the following comments:

1) It is possible to produce negative pion beams of rather high intensity with field-down conditions of the machine, for high values of the MH1 current and by choosing a radial position of the pion producing internal target $\leq$ 225 cm.

2) The ratio of the number of pions to the number of electrons can be made of the order of two by acting on the MH1 current; the higher the current the lower the electron contamination.

3) The rather large width of the range curve is due to the energy spread of the incoming beam and can be reduced only by decreasing strongly the aperture of the collimator thereby causing a strong reduction in intensity. The correlation between the two conditions is clearly shown in Figures 10 and 11.

Measurements 1/1 and 1/2 in Table I differ from the preceding ones in the distance of the beam telescope from the output quadrupoles. In the measurement 1/1 the distance was equal to 4.80 meters; in the measurement 1/2 the distance was reduced to 2.60 meters, which will be the distance in the planned experiment. All the other measurements were taken at large distances to favour the application of the time-of-flight technique.

The good efficiency of the anticounter C_4 is shown in Figure 12, representing the number of $C_1 \times C_2 \times C_3 \times \bar{C}_4$ coincidences taken without any absorber. In this case the efficiency is 99.5%. This is not in disagreement with the ratio peak-to-valley found in the range curve of Figure 5 because the two curves are taken in different experimental conditions. The spread in momentum $\Delta p/p$ (6%) is such that in our 0.2 gr/cm^2 counter C_3 only about 4% of the incident pion beam, already reduced by 12% the absorber, can be stopped. After careful examination of all these results our choice was the solution 1/2 Table I.

TABLE N° 1

MEASURE NUMBER	MAGNET CURRENT (AMPERE) MH1	LC1	LC2	LB30	LB31	MC3	LB40	LB25	TARGET POSITION AZIMUTH (DEGREES)	RADIUS (cm)	$C_1 \times C_2$ COUNTING RATE ($\times 10^3$ sec^{-1})	RATIOS OF T.O.F. PEAK AREAS $\frac{\pi^-}{e^-}$	$\frac{\mu^-}{e^-}$	PIONS STOPPING RATE (sec^{-1})	RANGE CURVE PEAK-TO-VALLEY RATIO FWHM (gr/cm^2) Al THICKNESS (cm)	π^- ENERGY (MEV) MEASURED CALCULATED	μ^- ENERGY (MEV) MEASURED CALCULATED
1 FIELD-DOWN	396 ↑	286 ↑	250 ↓	180 ↓	185 ↑	150 ↓	185 ↓	200 ↑	23.44	226.5	28.0	2.62	.70	520	8.23 5.07 10.7	97. 108.	112.5 124.0
2 FIELD-UP	90 ↑	328 ↑	295 ↓	197 ↓	185 ↑	168.5 ↓	285 ↓	212 ↑	13.42	223.5	19.0	2.23	.55	1274 WITH ^{12}C	8.18 4.63 13.5	116. 122.	132. 145.
3 FIELD-DOWN	400 ↑	290 ↑	0 ↓	190 ↓	180 ↑	169 ↓	185 ↓	10 ↑	23.44	225.0	150.0	1.11	.34	850	1.46 7.56 14.0	117. 123.	132.5 146.
4 FIELD-DOWN	400 ↑	280 ↑	290 ↓	200 ↓	205 ↑	180 ↓	250 ↓	250 ↑	17.5	226.0	23.0	3.37	.70	190	3.07 6.68 14.2 + 5.4 cm C_2H_2	122.5 134.5	138. 151.
5 FIELD-DOWN	360 ↑	325 ↑	285 ↓	315 ↓	300 ↑	190 ↓	240 ↓	240 ↑	23.0	225.5	14.5	5.54	1.51	740	286 6.37 15.8 + 8.1 cm C_2H_2	133. 145.	152. 164.
1/1 FIELD-DOWN	420 ↑	270 ↑	300 ↓	350 ↓	300 ↑	152 ↓	420 ↓	345 ↑	23.0	225.0	—	1.61	.58	310	5.06 4.68 12.0	108. 116.	124. 135.
1/2 FIELD-DOWN	410 ↑	260 ↑	292 ↓	200 ↓	190 ↑	150 ↓	300 ↓	290 ↑	23.0	225.0	250	—	—	8000	2.95 7.3 12.2	108. 116.	124. 135.

REFERENCES

(1) C. Cernigoi, I. Gabrielli, N. Grion, G. Pauli and G. Moschini, R. A. Ricci: "Proposal to study the absorption of at rest in ^{4}He, ^{9}Be, ^{12}C, ^{14}N, and ^{16}O" Doc. CERN/SCC/76-18 SCC/P, Doc. CERN/SCC 76-4, 1 Mar. 1976.

(2) C. Cernigoi, N. Grion, G. Pauli and B. Saitta: "Preliminary results on the time resolution of a plastic scintillator neutron counter of large area for neutrons of 16 MeV" accepted for publication by Nucl. Instr. and Meth. (1977).

(3) C. Cernigoi, N. Grion and G. Pauli, "Timing with large area plastic scintillator counters", Nucl. Instr. and Meth., 131 (1975) 495.

FIGURE CAPTIONS

Figure 1 - Lay-out of the experimental area.

Figure 2 - Beam telescope.

Figure 3 - Block diagram of the electronics.

Figure 4 - Time-of-flight spectrum and time calibration for field-down conditions of the machine and MC3 current equal to 152 A.

Figure 5 - Range curve for MC3 current of 152 A.

Figure 6 - Time-of-flight spectrum with the 457 Biased Time-to-Pulse--Height Converter gated by the $C_1 \times C_2 \times C_3 \times \bar{C}_4$ coincidence and with electron contamination.

Figure 7 - Time-of-flight spectrum with the 457 Biased Time-to-Pulse--Height Converter gated by the $C_1 \times C_2 \times C_3 \times \bar{C}_4$ coincidence and without electron contamination.

Figure 8 - Range curve with (dashed line) and without (solid line) electron contamination.

Figure 9 - Stopping rate of negative pions as a function of the MC3 current.

Figure 10 - Stopping rate of negative pions as a function of the horizontal collimator aperture and schematic representation of the collimator.

Figure 11 - FWHM of the range curve as a function of the horizontal collimator aperture.

Figure 12 - Delay curve of the $C_1 \times C_2 \times C_3 \times \bar{C}_4$ coincidence.

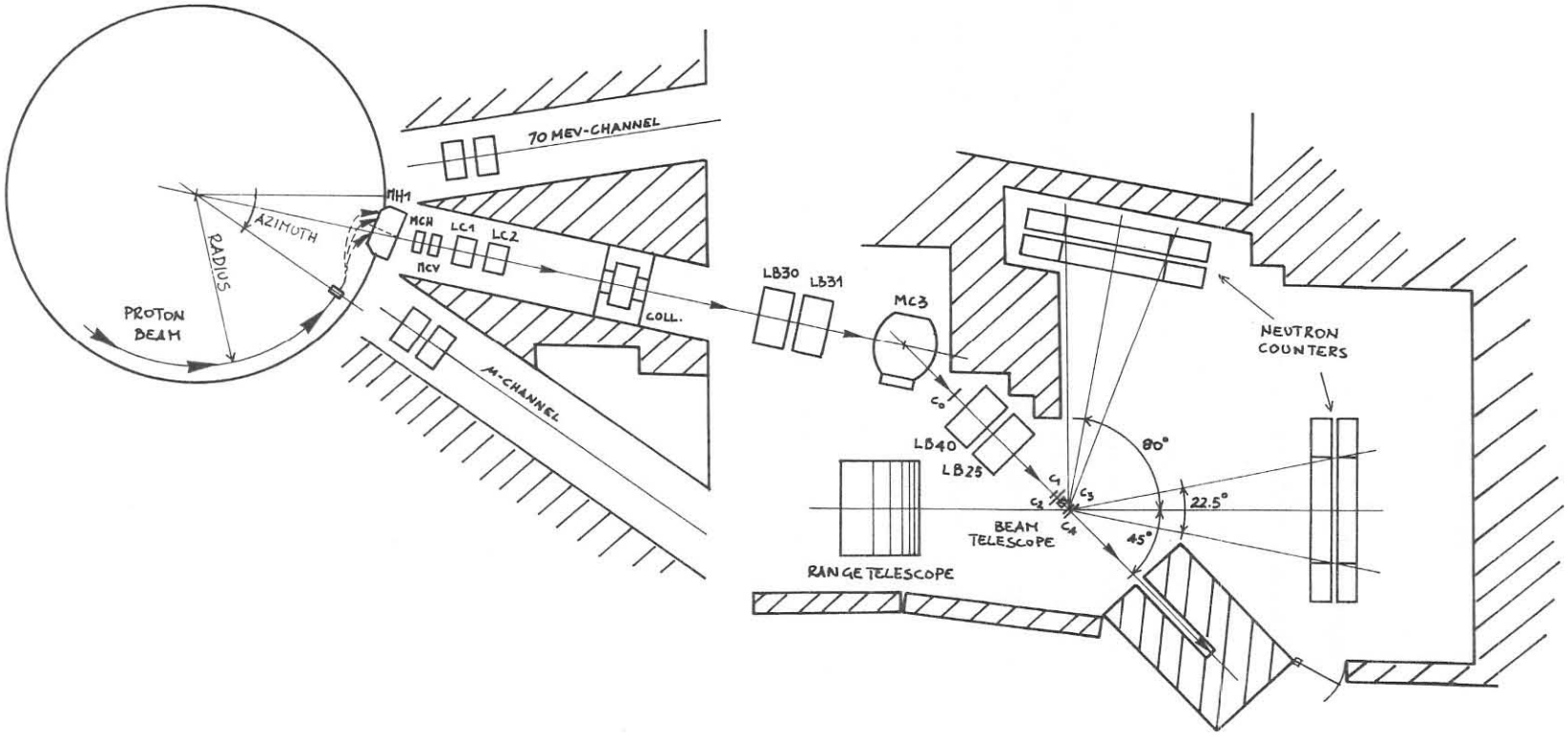

FIG. 1 : LAY-OUT OF THE EXPERIMENTAL AREA

FIG. 2 : BEAM TELESCOPE

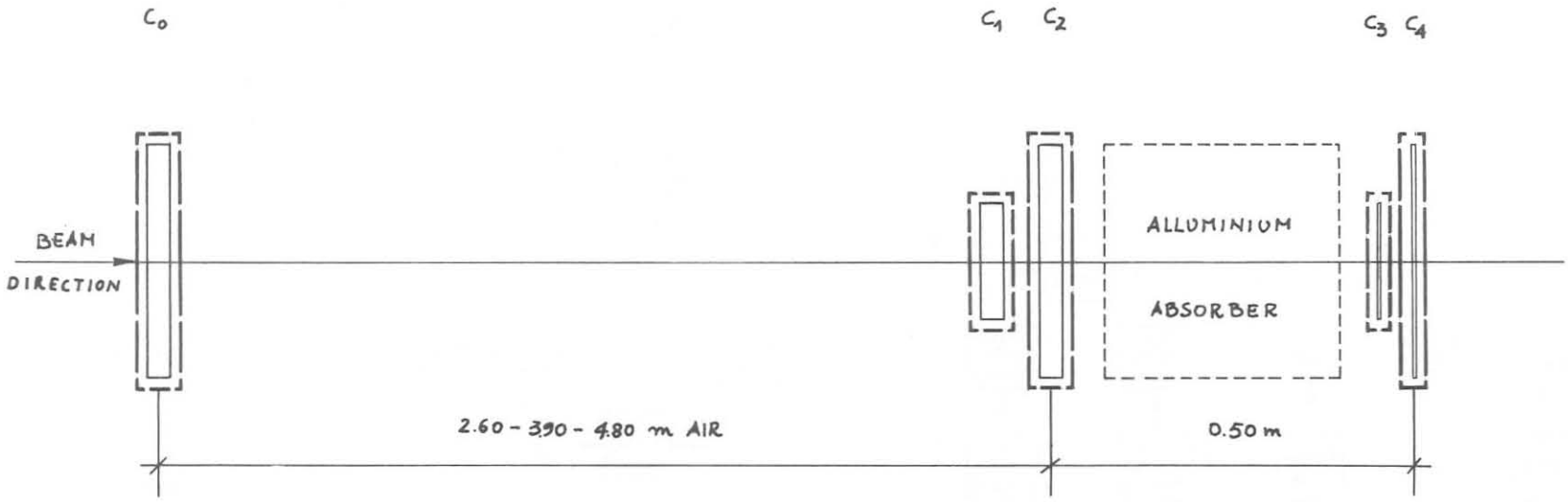

C_0, C_2 :	NE111 PLASTIC SCINTILLATOR	($10\times10\times1$ cm^3)	WITHOUT	ALUMINIUM	WRAPPING
C_1 :	NE104 PLASTIC SCINTILLATOR	($10\times10\times1$ cm^3)	"	"	"
C_3 :	NE104 PLASTIC SCINTILLATOR	($10\times10\times0.2$ cm^3)	"	"	"
C_4 :	NE104 PLASTIC SCINTILLATOR	($30\times20\times0.5$ cm^3)	WITH	ALUMINIUM	WRAPPING

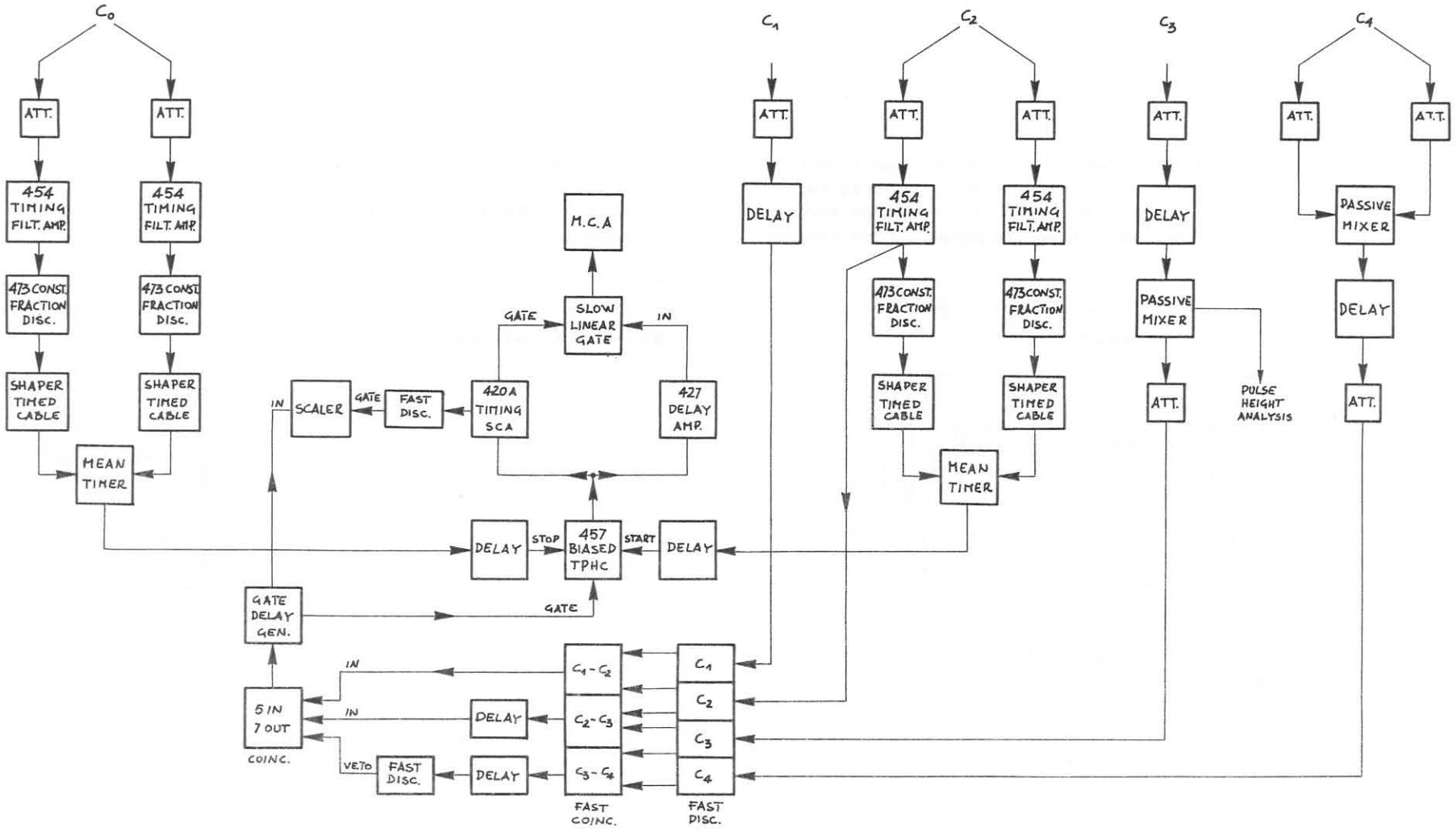

FIG. 3 : BLOCK DIAGRAM OF THE ELECTRONICS

FIG. 4 : T.O.F. SPECTRUM AND CALIBRATION FOR MC3 CURRENT = 152A

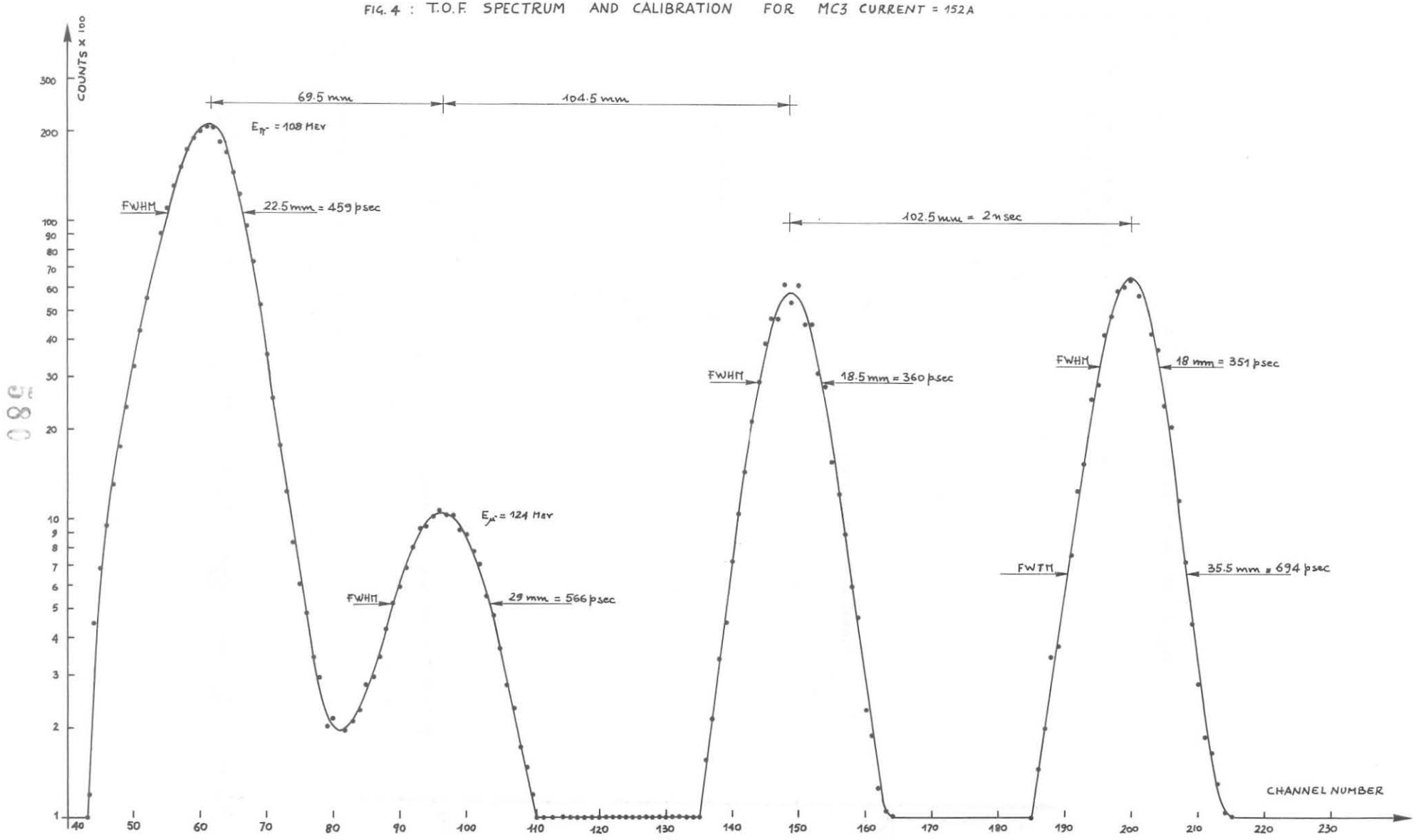

FIG. 5 : RANGE CURVE FOR $MC_3 = 152$ A

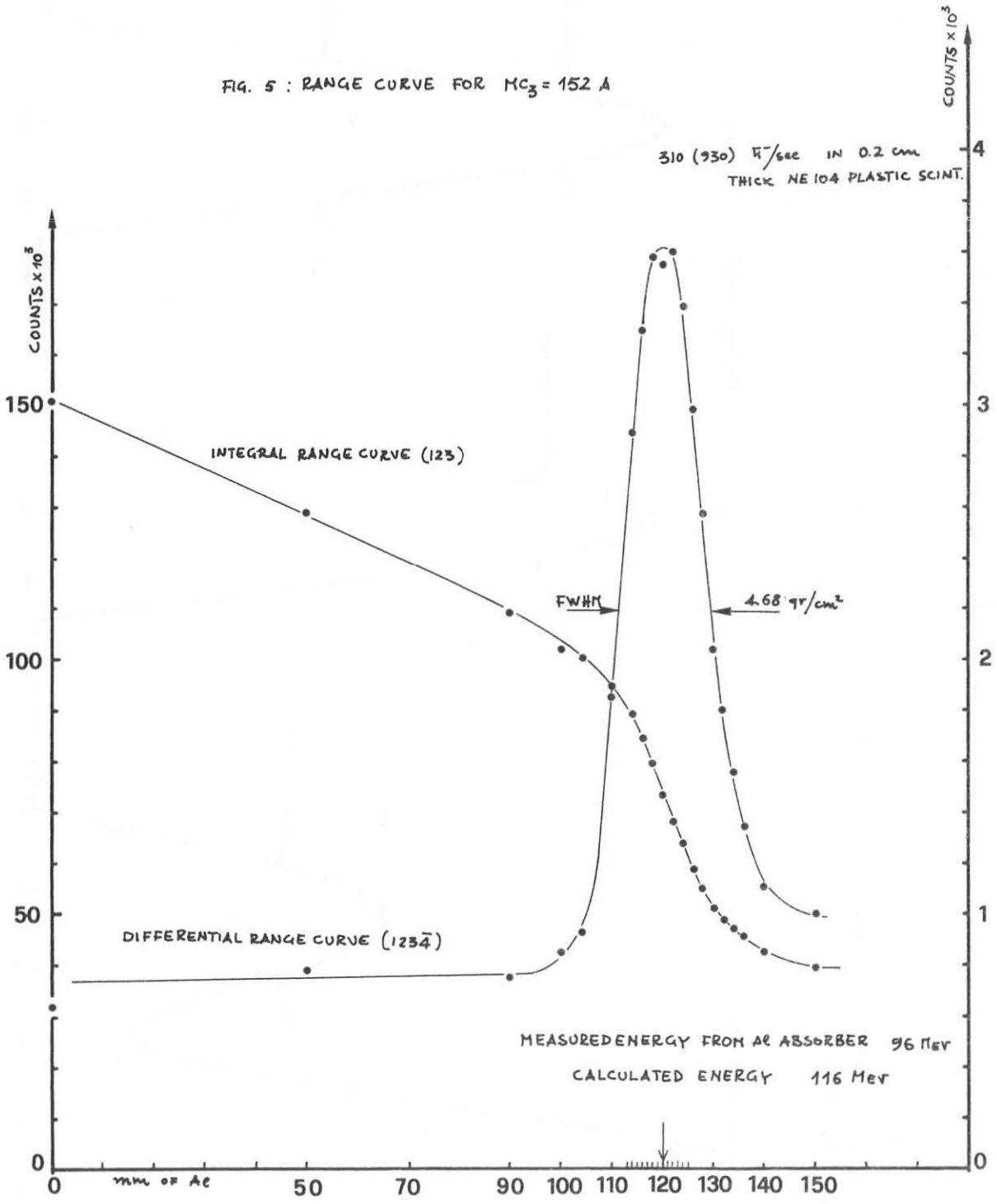

FIG. 6 : T.O.F. SPECTRUM WITH ELECTRON CONTAMINATION

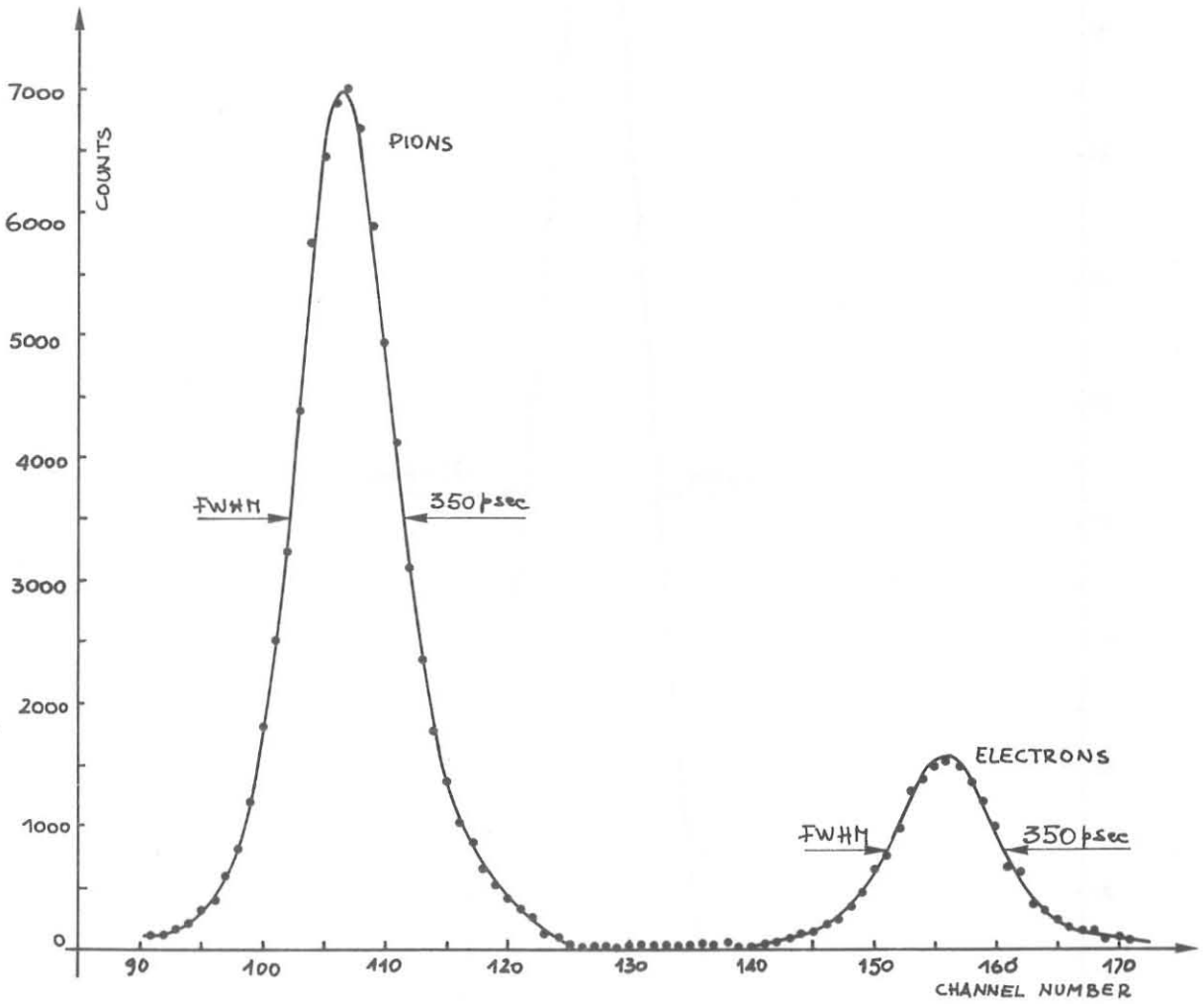

FIG. 7 : T.O.F. SPECTRUM WITHOUT ELECTRON CONTAMINATION

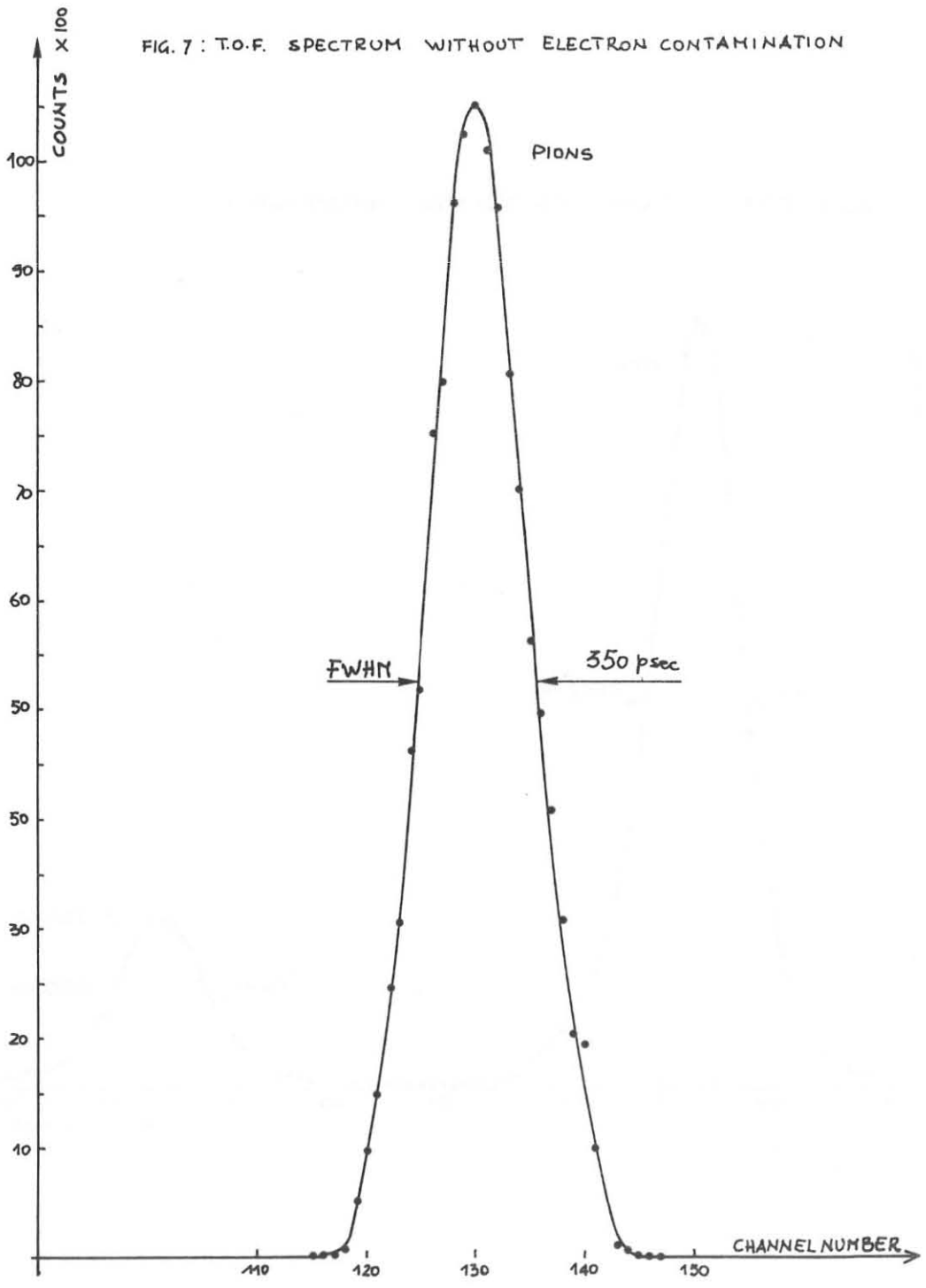

FIG. 8 : RANGE CURVES FOR $MC_3 = 150A$

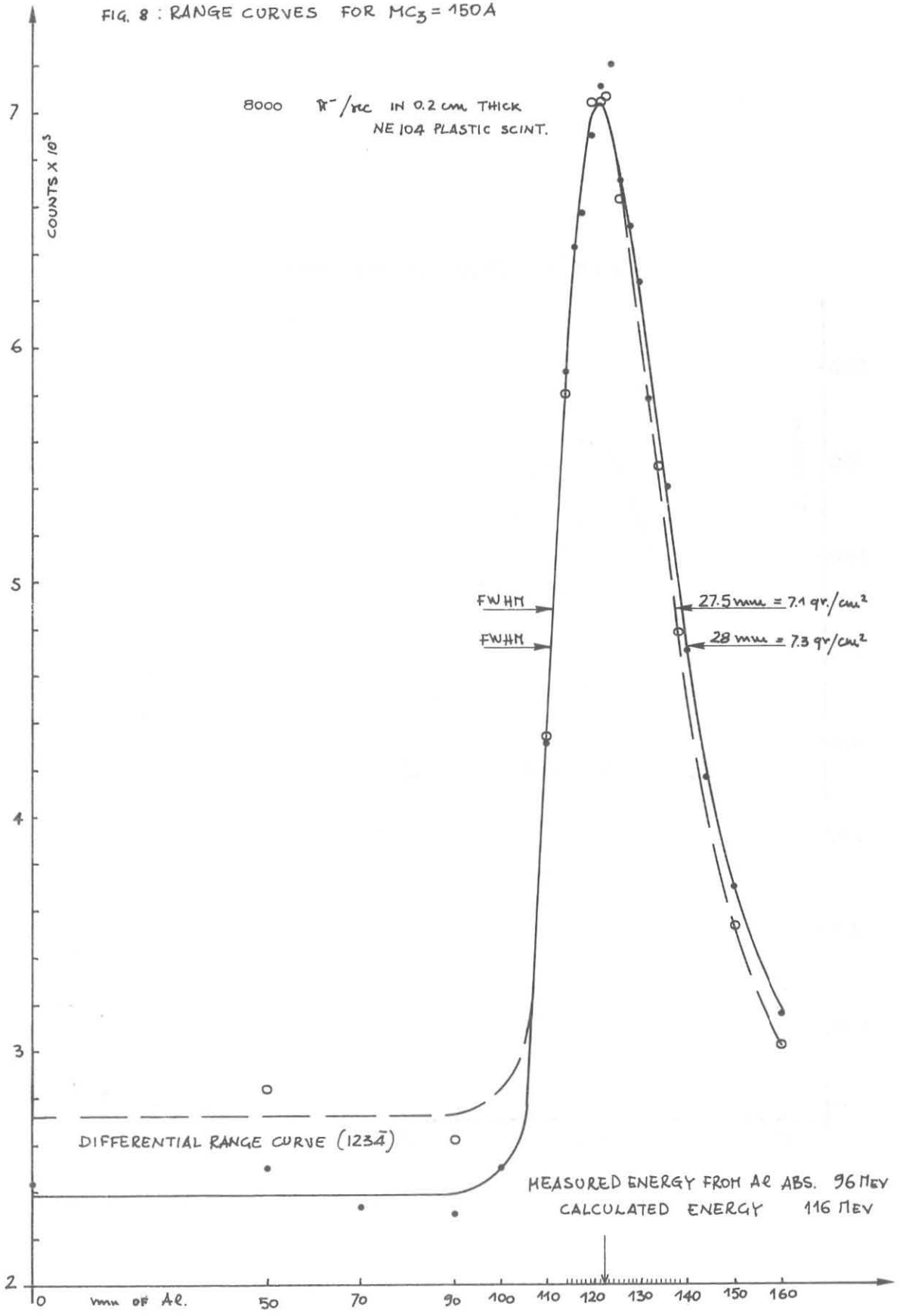

FIG. 9 : π^- STOP/sec VS MC3 CURRENT

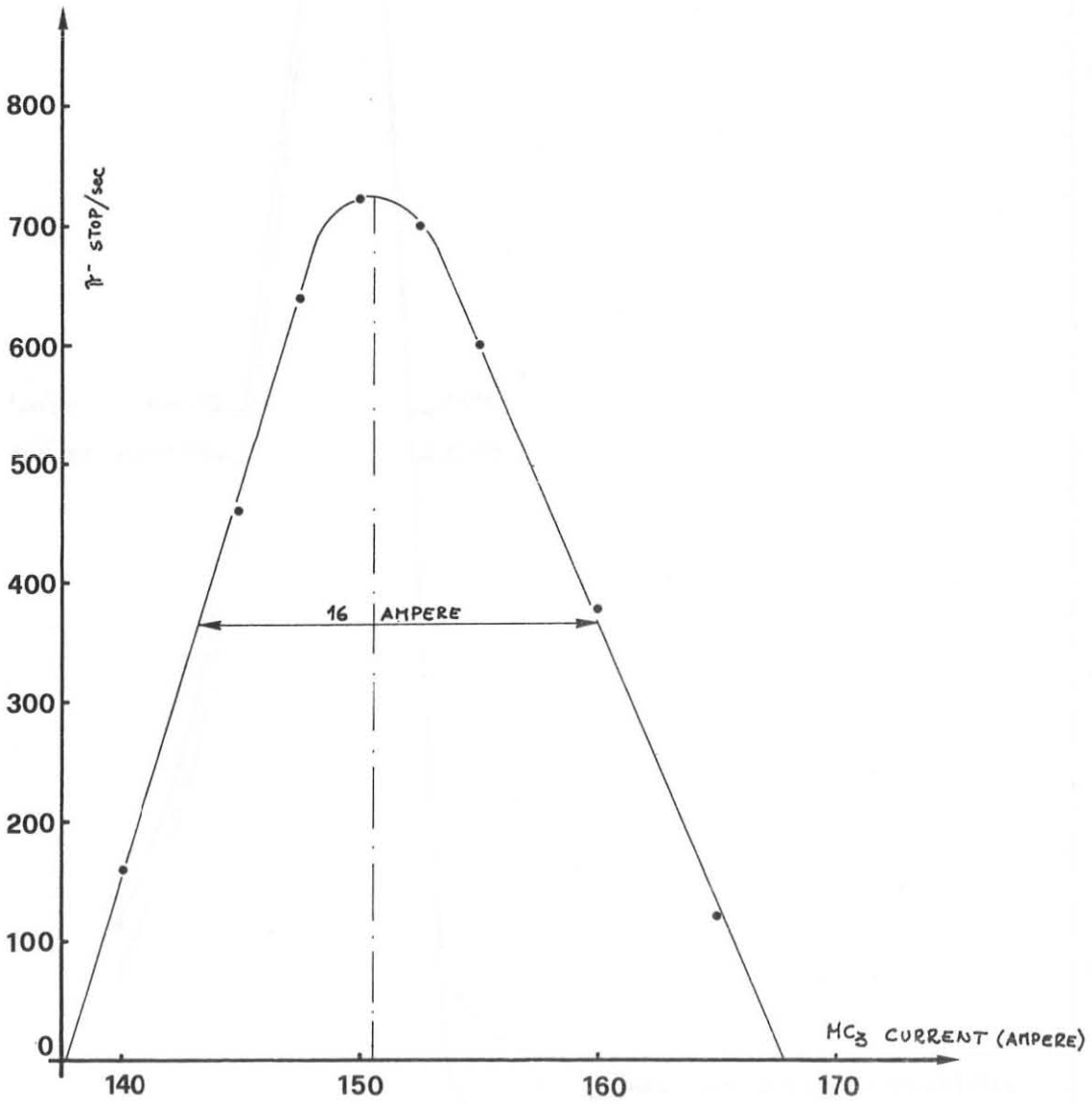

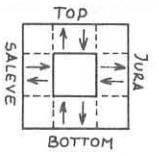

FIG. 10 : STOPPED PIONS VS HORIZONTAL COLLIMATOR APERTURE

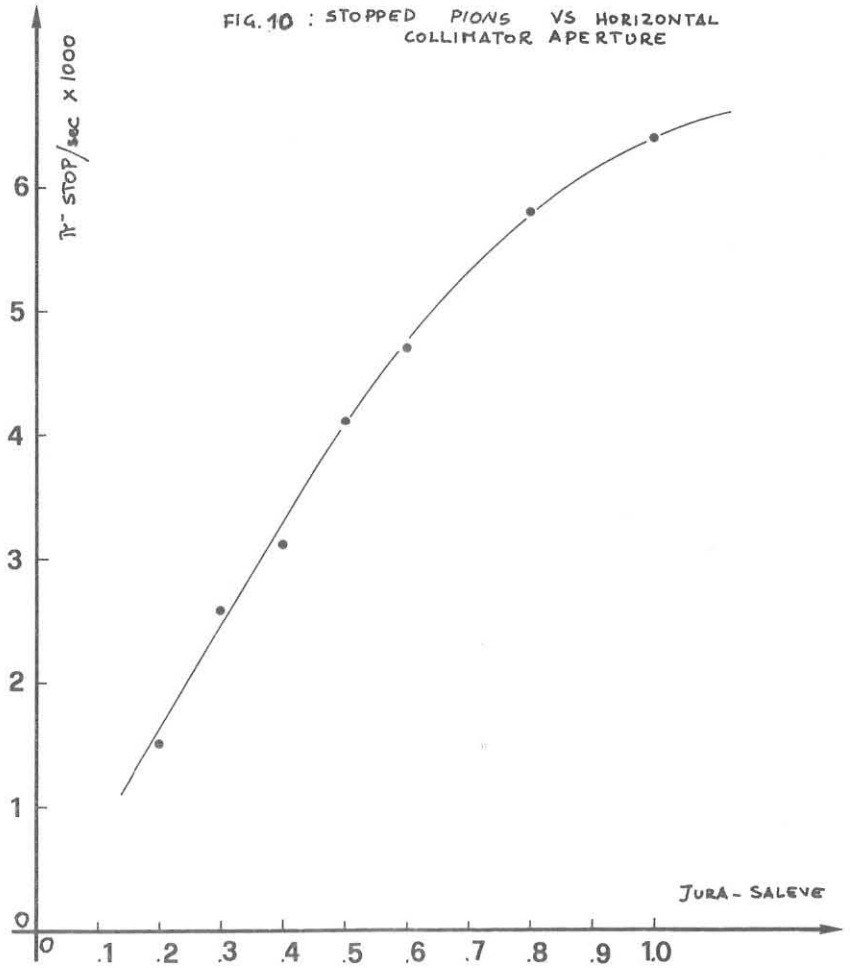

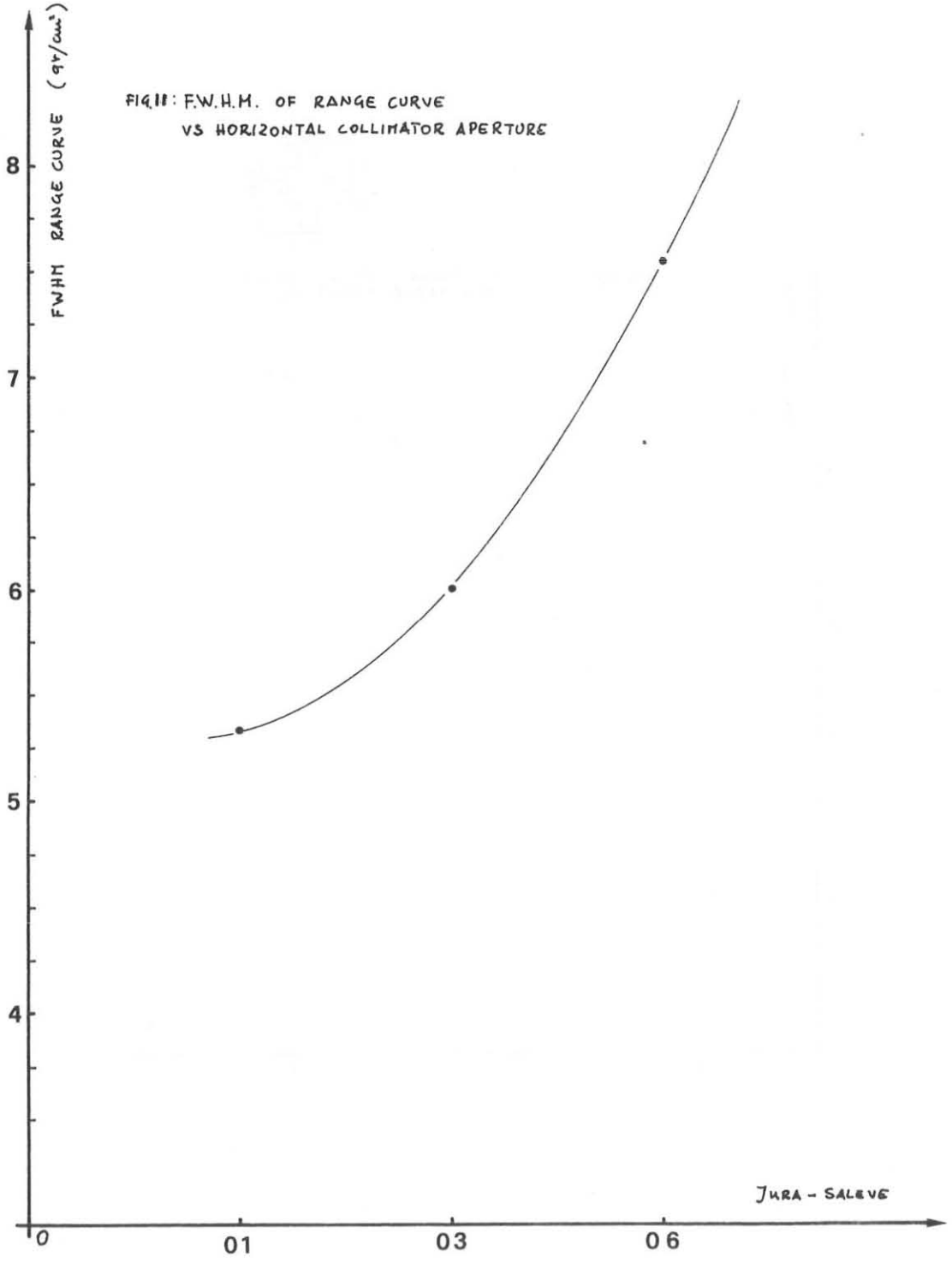

FIG 11 : F.W.H.M. OF RANGE CURVE
VS HORIZONTAL COLLIMATOR APERTURE

FIG. 12

DELAY CURVE OF THE $123\bar{4}$ COINCIDENCE